POLA-01

Kinetic modeling of auroral ion Outflows observed by the VISIONS sounding rocket

R. M. Albarran[1], M. Zettergren[1]

Embry-Riddle Aeronautical University[1]

EMBRY-RIDDLE Aeronautical University

The VISIONS (VISualizing Ion Outflow via Neutral atom imaging during a Substorm) sounding rocket was launched on Feb. 7, 2013 at 8:21 UTC from Poker Flat, Alaska, into an auroral substorm with the objective of identifying the drivers and dynamics of the ion outflow below 1000km. Energetic ion data from the VISIONS polar cap boundary crossing show evidence of an ion "pressure cooker" effect whereby ions energized via transverse heating in the topside ionosphere travel upward and are impeded by a parallel potential structure at higher altitudes. VISIONS was also instrumented with an energetic neutral atom (ENA) detector which measured neutral particles (∼50-100 eV energy) presumably produced by charge-exchange with the energized outflowing ions. Hence, inferences about ion outflow may be made via remotely-sensing measurements of ENAs. This investigation focuses on modeling energetic outflowing ion distributions observed by VISIONS using a kinetic model. This kinetic model traces large numbers of individual particles, using a guiding-center approximation, in order to allow calculation of ion distribution functions and moments. For the present study we include mirror and parallel electric field forces, and a source of ion cyclotron resonance (ICR) wave heating, thought to be central to the transverse energization of ions. The model is initiated with a steady-state ion density altitude profile and Maxwellian velocity distribution characterizing the initial phase-space conditions for multiple particle trajectories. This project serves to advance our understanding of the drivers and particle dynamics in the auroral ionosphere and to improve data analysis methods for future sounding rocket and satellite missions.

Motivation

The ionosphere plays a significant role in loading the magnetosphere plasma populations (Zeng, [2008]). Moreover, the energization and outflow of ions in the polar ionosphere was first observed by Shelley et al. in 1972 and has been reported by other satellite missions and simulation models (Retterer, [1983], Crew [1990]). Unlike the strongly field-aligned beam distributions generated in the dayside cleft/cusp, the ion conic formations in the cusp have peak fluxes at a pitch angle relative the field-aligned directions. The conic formation in velocity space is thought to be generated by gradual heating of ions. In this study, we present ion conic distributions generated by a 3D kinetic ion model with ICR wave heating. This model is used to reconstruct ENA trajectories and ion outflow source regions as observed by satellites and sounding rockets - and in this case the VISIONS sounding rocket.

Magnetic Dipole Coordinates

The Earth's magnetic dipole field is with no free currents and spherical boundary conditions $\Phi_B \to 0$ as $r \to \infty$ and $\Phi_B \to \infty$ as $r \to 0$ is given by

$$\mathbf{B} = \left[\frac{2m\cos(\theta)}{r^3}\right]\hat{\mathbf{e}}_\mathbf{r} + \left[\frac{m\sin(\theta)}{r^3}\right]\hat{\mathbf{e}}_\theta$$

where $B = |\mathbf{B}| = \frac{m\sqrt{\ell}}{r^3}$, $\ell = 1+3\cos^2(\theta)$, $\mathbf{B} = B\hat{\mathbf{e}}_\mathbf{q}$, $r = R_0\sin^2(\theta)$ and $\theta = \arcsin\left(\sqrt{r/R_0}\right)$. The dipole coordinate system $(q,\ p,\ \theta_d)$ has q along the field line, p as the L-shell, and θ_d the dipole longitude.

$$q = \frac{R_E^2\cos(\theta)}{r^2} = \frac{R_E^2\cos(\theta)}{R_0^2\sin^4(\theta)}, \qquad p = \frac{r}{R_E\sin^2(\theta)} = \frac{R_0}{R_E}, \qquad \phi_d = \phi,$$

where $m = \mu_0 M_0 R_E^3/3 = B_E R_E^3$, $\mathbf{M} = M_0\hat{\mathbf{e}}_\mathbf{z}$ is Earth's magnetic moment, $B_E = m/r^3$ is B at equator ($\theta = \pi/2$), R_E is Earth's equatorial radius and R_0 is distance to dipole field line at equator.

The kinetic equations of motion of this model are performed in Cartesian unit basis $(\hat{\mathbf{e}}_\mathbf{x},\ \hat{\mathbf{e}}_\mathbf{y},\ \hat{\mathbf{e}}_\mathbf{z})$ to avoid time-dependent unit vectors, although, the forces are developed in magnetic dipole coordinates $(\hat{\mathbf{e}}_\mathbf{q},\ \hat{\mathbf{e}}_\mathbf{p},\ \hat{\mathbf{e}}_{\phi_\mathbf{d}})$. The Cartesian and dipole systems are related via the spherical coordinate system $(\hat{\mathbf{e}}_\mathbf{r},\ \hat{\mathbf{e}}_\theta,\ \hat{\mathbf{e}}_\phi)$, where $\ell = 1+3\cos^2(\theta)$:

$$\hat{\mathbf{e}}_\mathbf{x} = \left[3\cos(\theta)\sin(\theta)\cos(\phi)/\sqrt{\ell}\right]\hat{\mathbf{e}}_\mathbf{q} + \left[\cos(\phi)(1-3\cos^2(\theta))/\sqrt{\ell}\right]\hat{\mathbf{e}}_\mathbf{p} + [\sin(\phi)]\,\hat{\mathbf{e}}_{\phi_\mathbf{d}}$$

$$\hat{\mathbf{e}}_\mathbf{y} = \left[3\cos(\theta)\sin(\theta)\sin(\phi)/\sqrt{\ell}\right]\hat{\mathbf{e}}_\mathbf{q} + \left[\sin(\phi)(1-3\cos^2(\theta))/\sqrt{\ell}\right]\hat{\mathbf{e}}_\mathbf{p} - [\cos(\phi)]\,\hat{\mathbf{e}}_{\phi_\mathbf{d}}$$

$$\hat{\mathbf{e}}_\mathbf{z} = \left[(3\cos^2(\theta)-1)/\sqrt{\ell}\right]\hat{\mathbf{e}}_\mathbf{q} + \left[3\cos(\theta)\sin(\theta)/\sqrt{\ell}\right]\hat{\mathbf{e}}_\mathbf{p}$$

$$\hat{\mathbf{e}}_\mathbf{q} = \left[3\cos(\theta)\sin(\theta)\cos(\phi)/\sqrt{\ell}\right]\hat{\mathbf{e}}_\mathbf{x} + \left[3\cos(\theta)\sin(\theta)\sin(\phi)/\sqrt{\ell}\right]\hat{\mathbf{e}}_\mathbf{y} + \left[(3\cos^2(\theta)-1)/\sqrt{\ell}\right]\hat{\mathbf{e}}_\mathbf{z}$$

$$\hat{\mathbf{e}}_\mathbf{p} = \left[\cos(\phi)(1-3\cos^2(\theta))/\sqrt{\ell}\right]\hat{\mathbf{e}}_\mathbf{x} + \left[\sin(\phi)(1-3\cos^2(\theta))/\sqrt{\ell}\right]\hat{\mathbf{e}}_\mathbf{y} + \left[3\cos(\theta)\sin(\theta)/\sqrt{\ell}\right]\hat{\mathbf{e}}_\mathbf{z}$$

$$\hat{\mathbf{e}}_{\phi_\mathbf{d}} = \sin(\phi)\hat{\mathbf{e}}_\mathbf{x} - \cos(\phi)\hat{\mathbf{e}}_\mathbf{y}$$

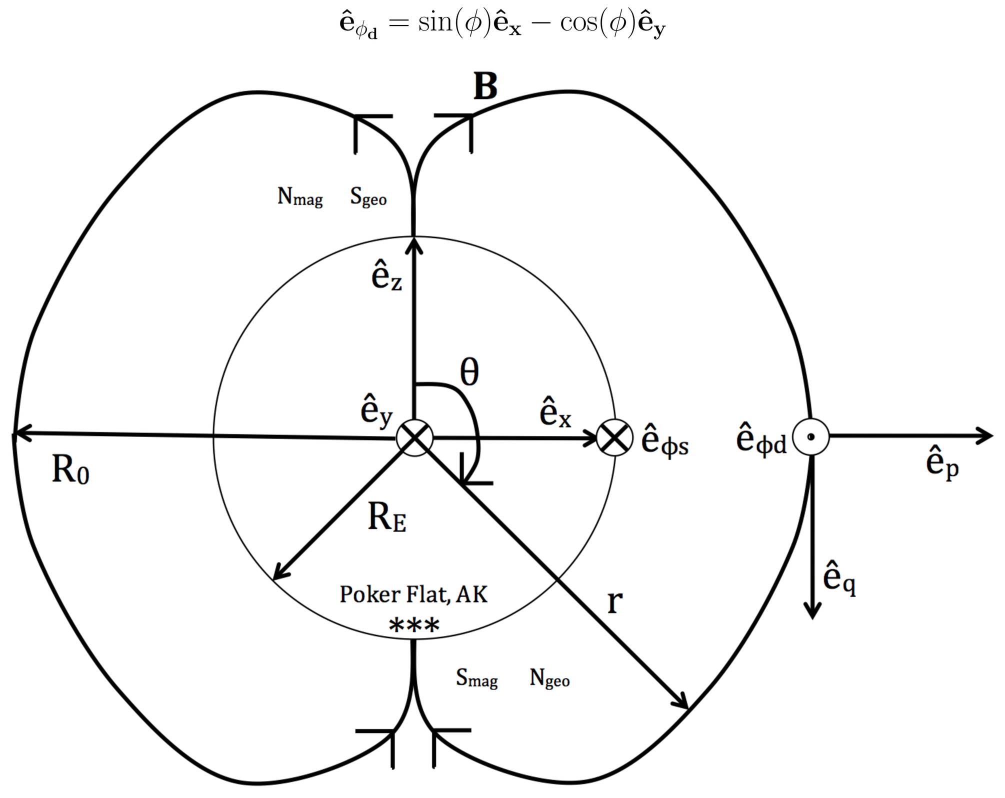

Figure 1: Configuration space in Cartesian, spherical, and magnetic dipole $(\hat{\mathbf{e}}_\mathbf{q},\ \hat{\mathbf{e}}_\mathbf{p},\ \hat{\mathbf{e}}_{\phi\mathbf{d}})$ coordinates where R_E is the Earth radius, $r = R_0$ at the equator ($\theta = \pi/2$), and N_{mag} (S_{mag}), and N_{geo} (S_{geo}) are the North (South) magnetic and geographic poles, respectively.

Phase-Space Initialization

The guiding center kinetic model includes the magnetic mirror force $\mathbf{F}_\mathbf{M} = |\mathbf{F}_\mathbf{M}|\hat{\mathbf{e}}_\mathbf{q}$ and the field-aligned Earth's gravitational force $\mathbf{F}_\mathbf{G} = |\mathbf{F}_\mathbf{G}|\hat{\mathbf{e}}_\mathbf{q}$, where $\mathbf{F}_\mathbf{M} = m_i\mathbf{a}_\mathbf{M} = -\mu_m\partial_q B\hat{\mathbf{e}}_\mathbf{q}$, $\mu_m = mv_\perp^2/(2B)$ is the ion magnetic moment where $v_\perp$ is the perpendicular velocity component. The acceleration term that is integrated for particle velocity and position is thus

$$\mathbf{a} = \left\{3F_N\cos(\phi)\cos(\theta)\sin(\theta)/m_i\sqrt{\ell}\right\}\hat{\mathbf{e}}_\mathbf{x} + \left\{3F_N\sin(\phi)\cos(\theta)\sin(\theta)/m_i\sqrt{\ell}\right\}\hat{\mathbf{e}}_\mathbf{y} + \left\{F_N(3\cos^2(\theta)-1)/m_i\sqrt{\ell}\right\}\hat{\mathbf{e}}_\mathbf{z},$$

where $F_N = |\mathbf{F}_\mathbf{N}| = |\mathbf{F}_\mathbf{M}| + |\mathbf{F}_\mathbf{G}|$, and m_i is the ion mass.

Initial particles positions are allocated in each configuration space cell according to a normalized steady-state ion density profile in Cartesian coordinates. The roots of the following quartic polynomial transform these positions into dipole coordinates (Huba, [2000]):

$$q^2(r/R_E)^4 + p^{-1}(r/R_E) - 1 = 0$$

Initial velocities have an 3D Maxwellian distribution in Cartesian coordinates where the field-aligned components are $v_\parallel = v_q$ and $v_\perp = \sqrt{v_p^2 + v_{\phi_d}^2}$. This transformation gives an energetically relaxed ion conic distribution. When ICR heating is turned off, the distribution is a drifting Maxwellian with time, otherwise, $v_\perp$ is updated accordingly.

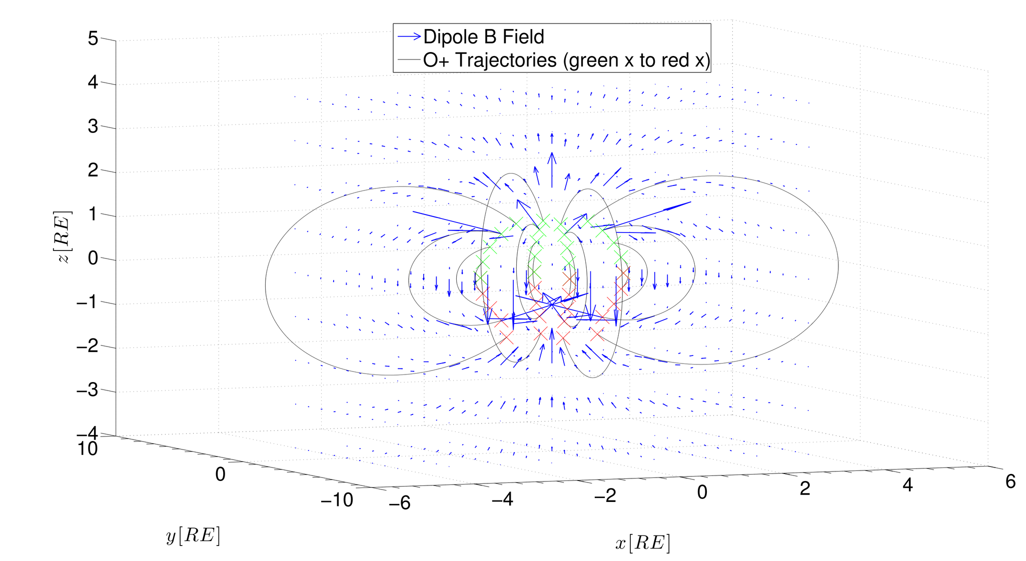

Figure 2: An example of O^+ ion motion by the mirror force along the dipole field.

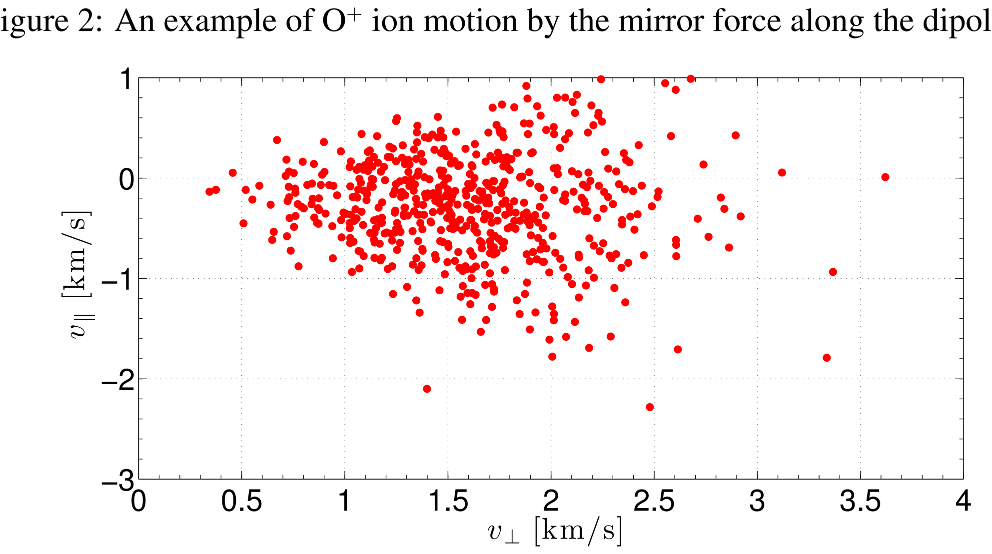

Figure 3: Initial field-aligned Maxwellian velocity distribution function before 250 second simulation duration.

3D Kinetic Solver

A fourth-order Runge-Kutta (RK4) scheme is employed to integrate the net acceleration components in Cartesian coordinates for the velocities and positions. The solver is conducted on a time domain $[A\ B]$ over N_t time-steps with a time-step of $h = (B-A)/N_t$. The solution is of order h^5. The ODE system is $a_i = \dot{v}_i$ where $a_i^n = a_i(x^n,\ y^n,\ z^n)$ with component index $i = x,\ y,\ z$ and time index n. According to the RK4 scheme:

$$k_1 = a_i^n = a_i(x^n,\ y^n,\ z^n), \qquad k_2 = a_i^{n+h/2} = a_i(x^{n+h/2},\ y^{n+h/2},\ z^{n+h/2}),$$
$$k_3 = a_i^{n+h/2} = k_2, \qquad k_4 = a_i^{n+h} = a_i(x^{n+h},\ y^{n+h},\ z^{n+h})$$

where

$$v_i^{n+1} = v_i^n + (h/6)(k_1 + 2k_2 + 2k_3 + k_4),$$

$i^{n+h} = i^n + hv_i^{n+h/2} = i^n + hv_i^n + (h^2/2)a_i^n\ \forall i = x,\ y,\ z$, where accelerations are computed given previous positions, where $a_i \neq a_i(v_i)$. To ensure a guiding center model, the Cartesian velocity components are recast into dipole velocity components where v_p is set to zero such that no particles overshoot the L-shell. In this study the L-shell difference is less than 10^{-3} of an R_E. A similar scheme is employed to solve $v_i = \dot{r}_i$.

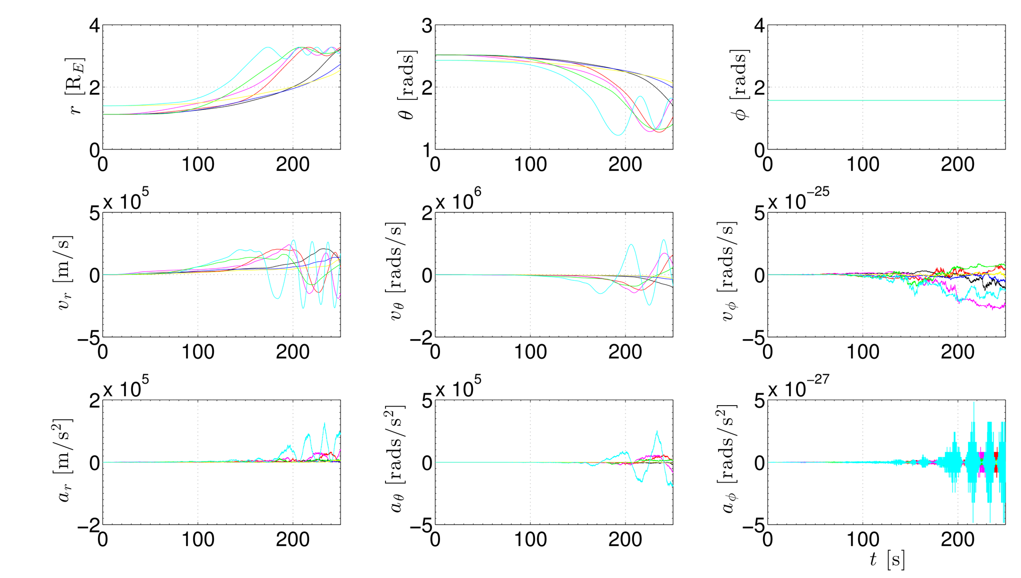

Figure 4: Spherical coordinate $(r,\ \theta,\ \phi)$ kinematics for arbitrarily selected particles.

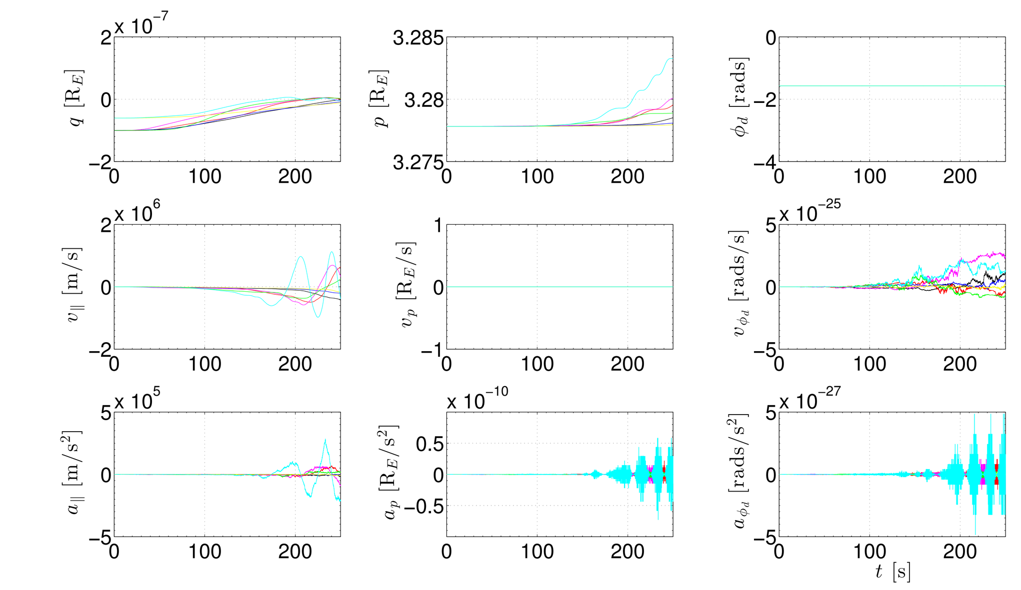

Figure 5: Dipole coordinate $(q,\ p,\ \phi_d)$ kinematics for arbitrarily selected particles, where p is the L-shell.

Ion Cyclotron Resonance Heating

Once the initial $v_\perp$ value is computed according to the initial Maxwellian velocity distribution, it is updated on every time-step as $v_\perp^{n+1} = \sqrt{(v_{\perp 1}^{n+1})^2 + (v_{\perp 2}^{n+1})^2}$ according to ICR heating by broad-band ELF waves, where $v_{\perp 1}^{n+1} = v_{\perp 1}^n + D_{V\perp 1}^n$, $v_{\perp 2}^{n+1} = v_{\perp 2}^n + D_{V\perp 2}^n$, $D_{V\perp 1}^n = \gamma_{\perp 1}^{n+1}\sqrt{2D_{\perp 1}^n h}$, $D_{V\perp 1}^n = \gamma_{\perp 2}^{n+1}\sqrt{2D_{\perp 2}^n h}$, and $\gamma_{\perp 1}$ and $\gamma_{\perp 2}$ are random numbers from a zero-mean Gaussian distribution. The variances of the distribution along $\hat{\mathbf{e}}_{\perp\mathbf{21}}$ and $\hat{\mathbf{e}}_{\perp\mathbf{2}}$ are $2D_{\perp 1}h$ and $2D_{\perp 2}h$, respectively. The perpendicular velocity diffusion coefficient $D_{\perp 1}$ along $\hat{\mathbf{e}}_{\perp\mathbf{1}}$ and associated heating rate $\dot{W}_{\perp 1} = 2m_i D_{\perp 1}$ (similarly along $\hat{\mathbf{e}}_{\perp\mathbf{2}}$) is:

$$D_{\perp 1} = \left(q_i^2/4m_i^2\right)\eta\chi_{\perp 1}|E_{\perp 0}|^2\left(\omega_g/\omega_{g0}\right)^{-\alpha_{\perp 1}} \qquad \dot{W}_{\perp 1} = \left(q_i^2/2m_i\right)\eta\chi_{\perp 1}|E_{\perp 0}|^2\left(\omega_g/\omega_{g0}\right)^{-\alpha_{\perp 1}}$$

$$D_{\perp 2} = \left(q_i^2/4m_i^2\right)\eta\chi_{\perp 2}|E_{\perp 0}|^2\left(\omega_g/\omega_{g0}\right)^{-\alpha_{\perp 2}} \qquad \dot{W}_{\perp 2} = \left(q_i^2/2m_i\right)\eta\chi_{\perp 2}|E_{\perp 0}|^2\left(\omega_g/\omega_{g0}\right)^{-\alpha_{\perp 2}}$$

where $\eta = 0.125$ is the fraction of BBELF wave power that is left-hand polarized, $\chi_{\perp 1}$ is the fraction of wave power along $\hat{\mathbf{e}}_{\perp\mathbf{1}}$, $|E_{\perp 0}|^2 = 0.3\,\mathrm{mV}^2\cdot\mathrm{m}^{-2}\cdot\mathrm{Hz}^{-1}$ is the total electric field spectral density, and $\alpha_{\perp 1} = \alpha_{\perp 2} = 1.7$ is the spectral index at a reference gyrofrequency of $\omega_{g0} = 2\pi 6.5$ Hz (Wu, [1999]).

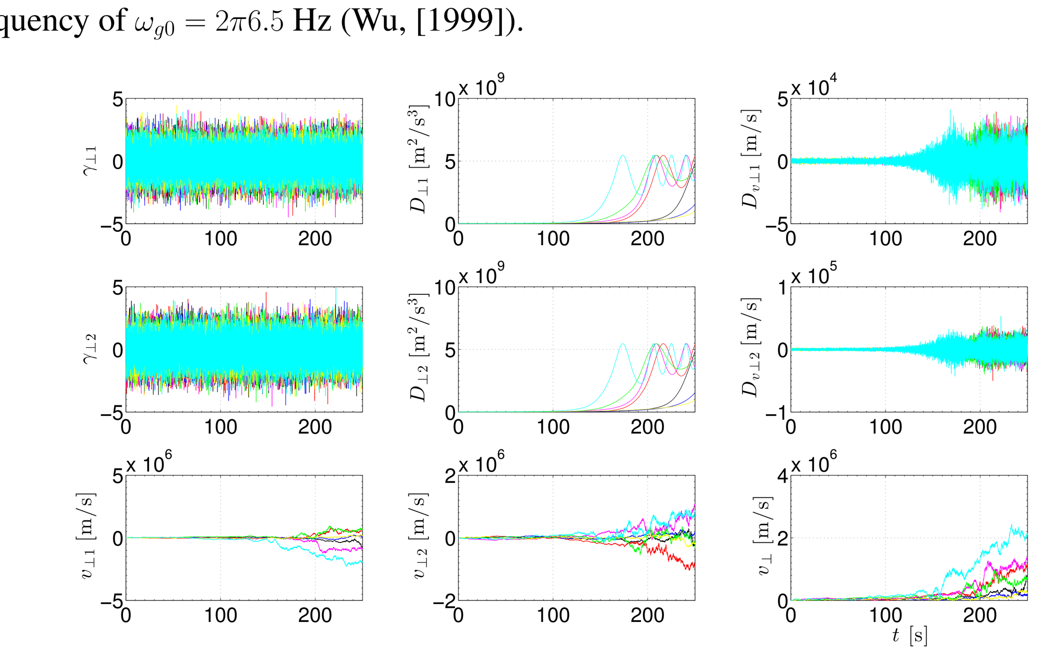

Figure 6: ICR heating parameters where $\gamma_{\perp 1}$ ($\gamma_{\perp 2}$) is a random number from a Gaussian distribution, $D_{\perp 1}$ ($D_{\perp 2}$) is the velocity diffusion coefficient, and $D_{V\perp 1}$ ($D_{V\perp 2}$) is the stochastic velocity kick along $\hat{\mathbf{e}}_{\perp\mathbf{1}}$ ($\hat{\mathbf{e}}_{\perp\mathbf{2}}$).

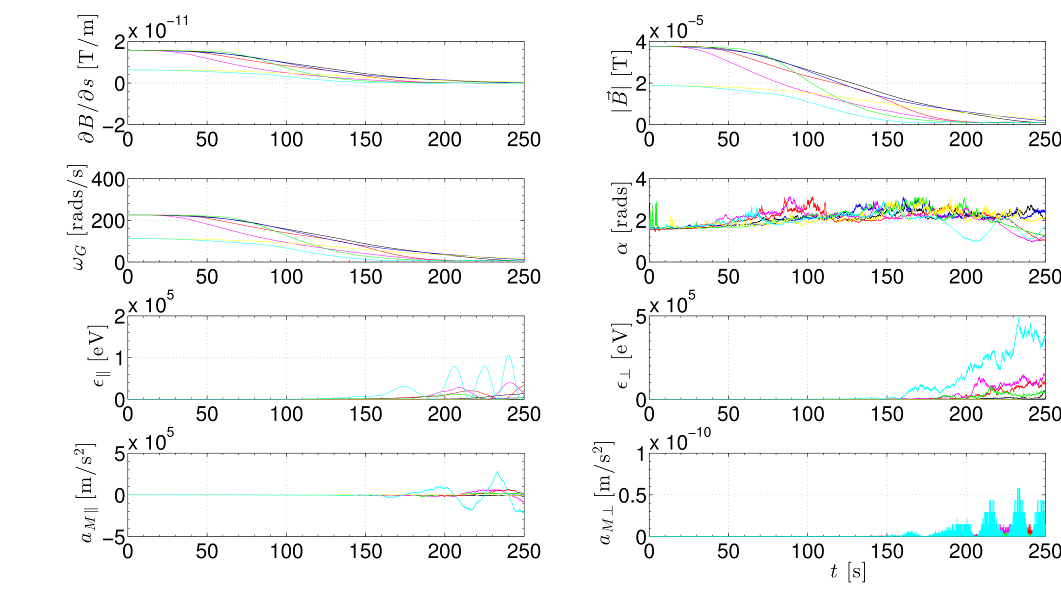

Figure 7: Mirror force parameters where $\partial B/\partial s$ it the field-aligned gradient of the magnetic field strength, $|\mathbf{B}|$, ω_G is the cyclotron frequency, α is particle pitch-angle, $\epsilon_\parallel$ ($\epsilon_\perp$) is the particle energy, and $a_{M\parallel}$ ($a_{M\perp}$) is the mirror force acceleration along $\hat{\mathbf{e}}_\parallel$ ($\hat{\mathbf{e}}_\perp$).

Conclusions & Future Work

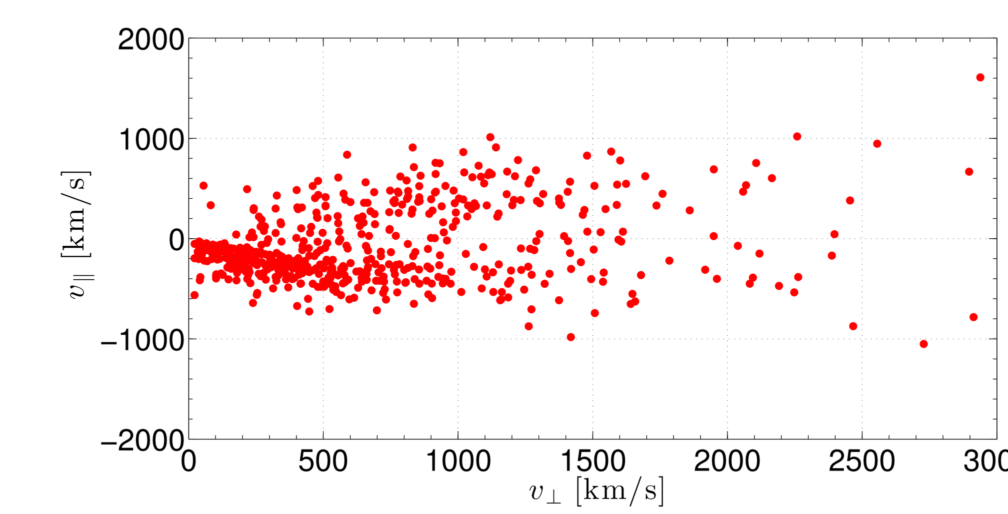

Figure 8: Final velocity-space distribution function after 250 second simulation duration.

The phase-space distributions generated in the presence of a magnetic mirror force, gravity, and ICR heating are ion conic (loss cone) distributions. Ion conics have been observed by in auroral passings of the Dynamics Explorer I satellite (Crew, [1990]), and replicated by numerical studies (Bouhram, [2003]). The source regions of ion outflow direct the trajectories of the ENAs detected by the VISIONS sounding rocket. Future work includes scaling the number of particles up to create smooth distributions functions with MPI and using a fluid electron energy equation solver to produce a downward parallel electric field consistent with the electron pressure. This ambi-polar electric field will be tested against the ICR heating to gauge the "pressure cooker" effect across the field-aligned potential structure. Ultimately, a 3D kinetic ENA model will be constructed to compliment this ion model. Virtual rockets flown through the computational domain will then lead to a reconstruction of the ENA source region and subsequent outflowing ion populations detected onboard.

References

- Crew, G. B., Chang, T., Retterer, J. M., "Ion Cyclotron Resonance Heated Conics: Theory and Observations," *Journal of Geophysical Research*, Vol. 95, No. A4, pp. 3959-3985, 1990
- Bouhram, M., Malingre, M., Jasperse, J. R., Dubouloz, N., Sauvaud, J.-A., "Modeling transverse heating and outflow of ionospheric ions from the dayside cusp/cleft. 2 Applications," *Annales Geophysicae*, Vol. 21, pp. 177-1791, 2003
- Retterer, J. M., "Ion Acceleration in the Superauroral Region: a Monte Carlo Model," *Geophysical Research Letters*, Vol. 10, No. 7, pp. 583-586, 1983
- Zeng, W., Horwitz, J. L., "Storm enhanced densities (SED) as possible sources for Cleft Ion Fountain dayside ionospheric outflows," *Geophysical Research Letters*, Vol. 35, 2008
- Wu, X.-Y., Horwitz, J. L., Estep, G. M., Su, Y.-J., Brown, D. G., Richards, P. G., "Dynamic fluid-kinetic (DyFK) modeling of auroral plasma outflow driven by soft electron precipitation and transverse ion heating," *Journal of Geophysical Research*, Vol. 104, No. A8, pp. 11263-17275, 1999

Acknowledgments

This poster was typeset in LaTeX.

Contact: **robert.albarran@my.erau.edu**